The 8th European Congress on Computational Methods in Applied Sciences and Engineering
ECCOMAS Congress 2022
5-–9 June 2022, Oslo, Norway

EFFICIENT DISPERSION CURVE COMPUTATIONS FOR PERIODIC VIBRO-ACOUSTIC STRUCTURES USING THE (GENERALIZED) BLOCH MODE SYNTHESIS

Vanessa Cool[1,2], Frank Naets[1,2], Lucas Van Belle[1,2], Wim Desmet[1,2] and Elke Deckers[2,3]

[1] KU Leuven, Department of Mechanical Engineering
Celestijnenlaan 300B - box 2420, 3001 Heverlee, Belgium

[2] DMMS lab, Flanders Make, Belgium

[3] KU Leuven Campus Diepenbeek, Department of Mechanical Engineering
Wetenschapspark 27, 3590 Diepenbeek , Belgium

Key words: periodic structures, vibro-acoustics, unit cell, model order reduction, dispersion curves

Abstract. Periodic structures such as metamaterials and phononic crystals hold potential as promising compact and lightweight solutions for noise and/or vibration attenuation in targeted frequency ranges. The performance of these structures is usually investigated by means of dispersion curves. The input for dispersion curve computations is often a finite element model of the corresponding unit cell. Nowadays, the vibration and noise attenuation of the periodic structures are generally tackled as separate problems and their performance is investigated with either structural or acoustic dispersion curves, respectively. Recently, vibro-acoustic unit cell models have come to the fore which can exhibit simultaneous structural and acoustic stopbands. However, the vibro-acoustic coupling inside the unit cell is usually not taken into account during the dispersion curve computations. To consider this coupling during their performance assessment, the computation of vibro-acoustic dispersion curves is required. Although these dispersion curves provide valuable information, the associated computational cost rapidly increases with unit cell model size. Model order reduction techniques are important enablers to overcome this high cost. In this work, the Bloch mode synthesis (BMS) and generalized BMS (GBMS) unit cell model order reduction techniques are extended to be applicable for 2D and 3D periodic vibro-acoustic systems. Through a verification case, the methodologies are shown to enable a strongly reduced dispersion curve calculation time while maintaining accurate predictions.

1 INTRODUCTION

In the search for lightweight and compact designs with favorable noise and vibration properties, periodic engineered structures have emerged which exhibit extraordinary properties not found in nature. These structures enable frequency ranges where wave attenuation takes place, called bandgaps. Two phenomena are commonly encountered: Bragg scattering leads to stop bands in phononic crystals, while Fano-type interference leads to stop bands in locally resonant

metamaterials [1]. The performance of these often periodic structures is analyzed with dispersion curves which give a relation between the frequency and wave propagation constant and thus contain information on the wave propagation in the corresponding infinite periodic structure. Therefore, the infinite periodic structure theory is applied, based on the smallest non-repetitive part, called the unit cell (UC), while applying the Bloch-Floquet theorem [2] to account for the periodicity. The UC model is often discretized using the finite element (FE) technique.

Nowadays, the vibration and noise attenuation of the periodic structures are generally tackled as separate problems resulting in either structural or acoustic phononic crystals or metamaterials. Their performance is, therefore, investigated with either purely structural or acoustic dispersion curves, respectively. Recently, vibro-acoustic UCs have come to the fore which (i) can obtain a simultaneous structural and acoustic bandgap [3, 4] or (ii) combine the structural and acoustic resonances [5] to exhibit extraordinary noise and vibration performance. However, in order to consider the possible vibro-acoustic coupling during the performance assessment, the computation of vibro-acoustic dispersion curves is required. Although including valuable information, the calculation of vibro-acoustic dispersion curves is cumbersome due to the nature of the vibro-acoustic system. Moreover the cost increases rapidly with the number of degrees-of-freedom (DOFs) in the UC and the number of required propagation constant evaluations for the dispersion curve calculation.

Model order reduction (MOR) techniques aim to overcome the high dispersion curve computation cost by constructing a reduced order UC model with less DOFs while preserving the important dynamic information. Several reduction techniques are available to accelerate the dispersion curve computation, ranging from wave-based to component mode synthesis-based techniques [6]. The Bloch mode synthesis (BMS) [7] and the generalized BMS (GBMS) [8] are the most commonly applied component mode synthesis techniques for the reduction of purely structural or acoustic UCs. They are Craig-Bampton methods and have as an advantage that the reduction of the UC happens without dependency on the wave propagation constants. The extension of the Craig-Bampton method for coupled vibro-acoustic structures was proposed in a substructuring context [9]. Recently, the applicability of the Craig-Bampton method is shown for the reduction of the interior and boundary DOFs for the calculation of frequency response functions of fluid-filled piping systems [10, 11].

In this work, the BMS and GBMS model reduction techniques are extended towards the reduction of vibro-acoustic 2D and 3D periodic UCs for the accelerated computation of vibro-acoustic dispersion curves. The efficiency and accuracy of the extended methodologies are investigated using a 2D vibro-acoustic UC model which contains a large number of DOFs.

This paper is structured as follows. Section 2 gives an overview of the vibro-acoustic FE UC model, dispersion curve calculation and introduces the extended BMS and GBMS model order reduction technique. In Section 3, the proposed methods are verified. The main conclusions are summarized in Section 4.

2 METHODOLOGY

This section first describes the dispersion curve calculation, after which the extended BMS and GBMS are presented. The theory is given for 2D periodic structures, while an extension towards 3D periodic structures can be done using [12].

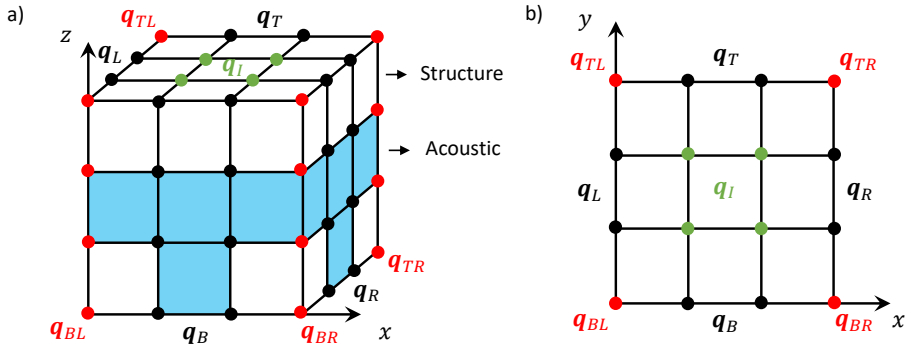

Figure 1: Schematic visualization of the node groups for a vibro-acoustic UC: a) three-dimensional view, b) top view.

2.1 Dispersion curve calculation

The input for the dispersion curve calculation is the UC model. In this work, vibro-acoustic UC designs are under consideration which are discretized using the $(\mathbf{u}, \mathbf{p})$ FE-formulation [13]:

$$\left(-\omega^2 \underbrace{\begin{bmatrix} \mathbf{M}_s & \mathbf{0} \\ \rho_a \mathbf{C}^T & \mathbf{M}_a \end{bmatrix}}_{\mathbf{M}} + \underbrace{\begin{bmatrix} \mathbf{K}_s & -\mathbf{C} \\ \mathbf{0} & \mathbf{K}_a \end{bmatrix}}_{\mathbf{K}} \right) \underbrace{\begin{bmatrix} \mathbf{u} \\ \mathbf{p} \end{bmatrix}}_{\mathbf{q}} = \underbrace{\begin{bmatrix} \mathbf{f}_s \\ \mathbf{f}_a \end{bmatrix}}_{\mathbf{f}}, \tag{1}$$

with $\mathbf{u}$ the displacement of the structural domain (subscript s), $\mathbf{p}$ the pressure of the acoustic domain (subscript a), $\mathbf{M}, \mathbf{K} \in \mathbb{R}^{N \times N}$ the mass and stiffness matrices, $\mathbf{C}$ the coupling matrix, ρ_a the density of the acoustic medium and ω the radial frequency. The UC DOFs are partitioned into interior and boundary ones (Fig. 1). Next, the Bloch-Floquet theorem [2] is applied on this UC to construct the characteristic dispersion eigenvalue problem which governs the wave propagation characteristics in the 2D infinite periodic structure:

$$(\tilde{\mathbf{K}} - \omega^2 \tilde{\mathbf{M}})\tilde{\mathbf{q}} = \mathbf{0}, \qquad \tilde{\mathbf{K}} = \mathbf{\Lambda}^H \mathbf{K} \mathbf{\Lambda}, \qquad \tilde{\mathbf{M}} = \mathbf{\Lambda}^H \mathbf{M} \mathbf{\Lambda}, \tag{2}$$

with H the Hermitian transpose, $\mathbf{\Lambda}$ the periodicity matrix and:

$$\mathbf{q} = \mathbf{\Lambda}\tilde{\mathbf{q}}, \quad \tilde{\mathbf{q}} = \begin{bmatrix} \mathbf{q}_I \\ \mathbf{q}_L \\ \mathbf{q}_B \\ \mathbf{q}_{BL} \end{bmatrix}, \quad \mathbf{\Lambda} = \begin{bmatrix} \mathbf{I} & \mathbf{0} & \mathbf{0} & \mathbf{0} \\ \mathbf{0} & \mathbf{\Lambda}_x & \mathbf{0} & \mathbf{0} \\ \mathbf{0} & \mathbf{0} & \mathbf{\Lambda}_y & \mathbf{0} \\ \mathbf{0} & \mathbf{0} & \mathbf{0} & \mathbf{\Lambda}_{x,y} \end{bmatrix}, \quad \mathbf{\Lambda}_i = \begin{bmatrix} \mathbf{I} \\ \lambda_i \mathbf{I} \end{bmatrix}, \quad \mathbf{\Lambda}_{i,j} = \begin{bmatrix} \mathbf{I} \\ \lambda_i \mathbf{I} \\ \lambda_j \mathbf{I} \\ \lambda_i \lambda_j \mathbf{I} \end{bmatrix}, \tag{3}$$

with $\tilde{\mathbf{q}}$ the periodic DOF vector and $\lambda_x = e^{j\mu_x}$, $\lambda_y = e^{j\mu_y}$ in which $\boldsymbol{\mu} = (\mu_x, \mu_y)$ is the propagation vector. In this work, the dispersion eigenvalue problem is solved using the $\omega(\boldsymbol{\mu})$-approach: a set of real $\boldsymbol{\mu}$ values is imposed and the problem is solved towards ω [1]. This results in free wave propagation solutions. The set of real $\boldsymbol{\mu}$-combinations are only selected along the Irreducible Brillouin Contour (IBC) of the UC [14]. In this work, Eq. (2) is solved in Matlab using the built-in function EIGS.

2.2 Model order reduction

The computational cost to solve Eq. (2) quickly increases with the number of DOFs and the number of imposed $\boldsymbol{\mu}$-pairs. This section elaborates on the extension of the BMS [7] and GBMS [8] unit cell reduction techniques towards vibro-acoustic UCs to accelerate this computation. The reduction techniques construct a projection basis $\mathbf{B} \in \mathbb{C}^{N \times N_B}$ using modal information and reduce the system matrices ($N_B \ll N$):

$$\mathcal{M} = \mathbf{B}^T \mathbf{M} \mathbf{B}, \qquad \mathcal{K} = \mathbf{B}^T \mathbf{K} \mathbf{B}. \tag{4}$$

After the transformation, the Bloch-Floquet boundary conditions (BCs) are imposed to construct the dispersion eigenvalue problem. Following sections discuss the construction of $\mathbf{B}$ in more detail for the BMS and GBMS technique.

2.2.1 Bloch mode synthesis

The BMS method reduces the (structural and acoustic) interior DOFs of the UC with a Craig-Bampton approach in which the interior DOFs are approximated as a linear combination of a set of fixed interface normal modes $\boldsymbol{\Phi}_I^t$ and a set of static constraint modes $\boldsymbol{\Psi}_{IA}^t$:

$$\begin{bmatrix} \mathbf{q}_I \\ \mathbf{q}_A \end{bmatrix} = \mathbf{B} \begin{bmatrix} \boldsymbol{\eta}_I \\ \mathbf{q}_A \end{bmatrix} = \begin{bmatrix} \boldsymbol{\Phi}_I^t & \boldsymbol{\Psi}_{IA}^t \\ \mathbf{0} & \mathbf{I} \end{bmatrix} \begin{bmatrix} \boldsymbol{\eta}_I \\ \mathbf{q}_A \end{bmatrix}, \tag{5}$$

in which the subscripts I and A represent the interior and boundary part of the UC, respectively, $\mathbf{q}_I \in \mathbb{R}^{N_I}$ and $\mathbf{q}_A \in \mathbb{R}^{N_A}$, and $\boldsymbol{\eta}_I$ is the reduced set of interior modal DOFs.

(i) $\boldsymbol{\Phi}_I^t$ is constructed using the coupled vibro-acoustic fixed interface normal modes. First the n_I smallest coupled modes ϕ_I^i are computed, after which these are partitioned into the structural and acoustic part:

$$\left(\mathbf{K}_{II} - \omega_i^2 \mathbf{M}_{II}\right) \phi_I^i = \mathbf{0}, \quad \phi_I^i = \begin{bmatrix} \phi_{s,I}^i \\ \phi_{a,I}^i \end{bmatrix}, \quad \boldsymbol{\Phi}_{j,I} = \begin{bmatrix} \phi_{j,I}^1 & \phi_{j,I}^2 & \dots & \phi_{j,I}^{n_I} \end{bmatrix}. \tag{6}$$

The partitioned modes are normalized, denoted by $\hat{\boldsymbol{\Phi}}_{j,I}$, to prevent singularity issues, leading to:

$$\boldsymbol{\Phi}_I^t = \begin{bmatrix} \hat{\boldsymbol{\Phi}}_{s,I} & \mathbf{0} \\ \mathbf{0} & \hat{\boldsymbol{\Phi}}_{a,I} \end{bmatrix}. \tag{7}$$

The N_I DOFs are reduced to $2n_I$ DOFs. In this work, a frequency-based truncation criterion for n_I is used: the modes up to four times the maximum frequency of interest are included.

(ii) The static constraint modes $\boldsymbol{\Psi}_{IA}^t$ represent the influence of the boundary motion on the interior part. To balance accuracy with computation speed, the static constraint modes are computed without taking into account any coupling [11]:

$$\boldsymbol{\Psi}_{s,IA} = -\mathbf{K}_{s,II}^{-1} \mathbf{K}_{s,IA}, \quad \boldsymbol{\Psi}_{a,IA} = -\mathbf{K}_{a,II}^{-1} \mathbf{K}_{a,IA}, \quad \boldsymbol{\Psi}_{IA}^t = \begin{bmatrix} \boldsymbol{\Psi}_{s,IA} & \mathbf{0} \\ \mathbf{0} & \boldsymbol{\Psi}_{a,IA} \end{bmatrix}. \tag{8}$$

Since the structural and acoustic boundary DOFs are kept as physical DOFs during the BMS reduction, the Bloch-Floquet BCs can straightforwardly be applied.

2.2.2 Generalized Bloch mode synthesis

The GBMS builds further upon the BMS technique and reduces also the boundary DOFs. An extra boundary transformation matrix $\mathbf{L}$ is constructed such that $\mathbf{q}_A = \mathbf{L}\boldsymbol{\eta}_A$, resulting in the reduction basis:

$$\begin{bmatrix}\mathbf{q}_I \\ \mathbf{q}_A\end{bmatrix} = \mathbf{B}\begin{bmatrix}\boldsymbol{\eta}_I \\ \boldsymbol{\eta}_A\end{bmatrix} = \begin{bmatrix}\boldsymbol{\Phi}_I^t & \boldsymbol{\Psi}_{IA}^t\mathbf{L} \\ \mathbf{0} & \mathbf{L}\end{bmatrix}\begin{bmatrix}\boldsymbol{\eta}_I \\ \boldsymbol{\eta}_A\end{bmatrix}. \tag{9}$$

The transformation matrix $\mathbf{L}$ is constructed using a truncated set of normal modes. The BMS reduced system matrices are first partitioned according to $\boldsymbol{\eta}_I$ and $\mathbf{q}_A$:

$$\left(\begin{bmatrix}\mathcal{K}_{II} & \mathcal{K}_{IA} \\ \mathcal{K}_{AI} & \mathcal{K}_{AA}\end{bmatrix} - \omega^2\begin{bmatrix}\mathcal{M}_{II} & \mathcal{M}_{IA} \\ \mathcal{M}_{AI} & \mathcal{M}_{AA}\end{bmatrix}\right)\begin{bmatrix}\boldsymbol{\eta}_I \\ \mathbf{q}_A\end{bmatrix} = \mathbf{0}. \tag{10}$$

Next, separate structural and acoustic boundary modes are computed, i.e. $i = s$ and a:

$$\left(\mathcal{K}_{i,AA} - \omega_j^2\mathcal{M}_{i,AA}\right)\phi_{i,A}^j = \mathbf{0}, \qquad \boldsymbol{\Phi}_{i,A} = \begin{bmatrix}\phi_{i,A}^1 & \phi_{i,A}^2 & \dots & \phi_{i,A}^{n_{i,A}}\end{bmatrix}, \qquad n_{i,A} \ll N_{i,A}, \tag{11}$$

$n_{s,A}$ and $n_{a,A}$ are determined to balance accuracy with speed [11]. Since the GBMS reduction is applied before the Bloch-Floquet BCs, the reduced modal boundary DOFs need to express the same compatibility conditions as the FOM. These conditions are enforced by partitioning the mode sets $\boldsymbol{\Phi}_{i,A}$ according to the different boundary parts, cf. Fig. 1. Next, the sets which require compatibility are combined and orthogonalized using a singular value decomposition to construct new bases $\boldsymbol{\Phi}_p$, with p representing the DOFs which are combined, e.g. $\boldsymbol{\Phi}_{s,lr}$ is the basis for the left and right structural boundary UC DOFs. All new bases are combined to construct the transformation matrix $\mathbf{L}$.

3 NUMERICAL VERIFICATION

This section verifies the proposed methodologies in terms of efficiency and accuracy on a 2D vibro-acoustic UC design. All calculations are performed on a laptop with 32 GB RAM and a 2.6 GHz Intel Core i7-9540 processor using Matlab R2019b. A relative frequency error is used to quantify the accuracy of the computed dispersion curves:

$$\epsilon_{rel} = \left|\frac{\omega_{ROM} - \omega_{FOM}}{\omega_{FOM}}\right|. \tag{12}$$

The vibro-acoustic 2D periodic UC design is taken over from Roca et al. [5] (Fig. 2). It consists of a hollow plate with a hollow pillar on top. All geometrical details and material properties can be found in [5]. It is opted to apply the UC with the pillar in the middle since this reduces the number of boundary DOFs which is favorable for the BMS and GBMS technique [15]. The UC is discretized using Simcenter NX with the FE method leading to 30238 DOFs of which 25476 structural and 4762 acoustic ones. The frequency range of interest goes from 0 Hz till 4500 Hz, leading to the calculation of the first 10 dispersion curves. The dispersion curves are computed along the IBC (Fig. 2b), with a resolution of 0.02π. The FOM dispersion curve calculation, which contains 27878 DOFs after applying the Bloch-Floquet BCs, requires 1446.1 s. The FOM vibro-acoustic and purely structural and acoustic dispersion curve are shown in Fig. 2c. The difference between the coupled and uncoupled dispersion curves indicates the vibro-acoustic coupling has a non-negligible effect.

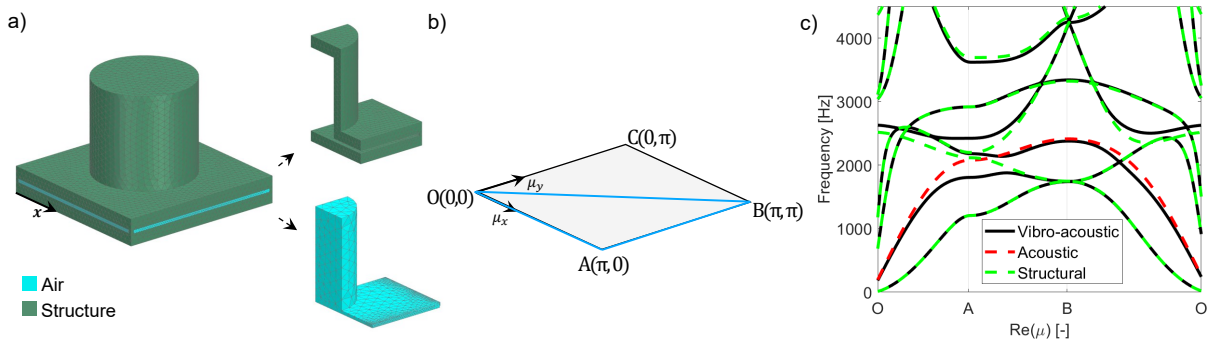

Figure 2: a) FE model of the vibro-acoustic 2D periodic UC with a detail of one fourth of the acoustic and structural part, b) IBC in reciprocal wave space, c) Coupled vibro-acoustic and uncoupled structural and acoustic FOM dispersion curves.

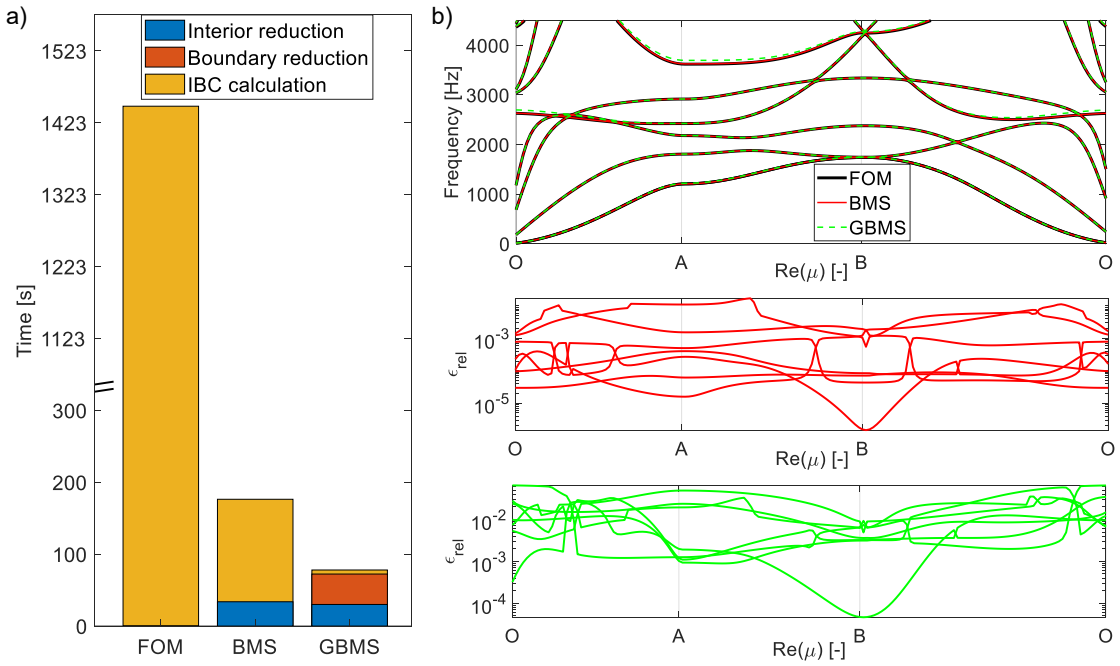

Figure 3: Results of the vibro-acoustic 2D periodic case. a) Comparison of the different calculation times for the construction of the ROM and the dispersion curve calculation. b) Dispersion curves of FOM and ROMs with corresponding relative error.

First of all, the BMS technique is applied with $n_I = 16$ which results in a ROM of 4716 DOFs, or 2356 DOFs after applying the Bloch-Floquet BCs. The construction of the ROM takes 33.82 s, while the dispersion curve computation takes 142.6 s (Fig. 3a). In total, this leads to an acceleration with factor 8.1 with respect to the FOM calculation. Fig. 3b shows the dispersion curves and corresponding relative errors. An accurate dispersion curve prediction is obtained with an error of $1.7 \cdot 10^{-2}$ or smaller.

Next, the dispersion curve calculation is further accelerated using the GBMS technique with $n_{s,A} = 120$ and $n_{a,A} = 30$. The number of considered modes is a trade-off between accuracy and speed. This results in a ROM with 894 DOFs, or 445 DOFs after applying the Bloch-Floquet BCs. The construction of the reduced model takes 102.4 s, while the dispersion curve calculation takes merely 5.6 s. This leads to an acceleration with factor 18.5 with respect to the FOM calculation. Fig. 3b shows the dispersion curves and corresponding relative errors. The relative error using the GBMS is slightly larger than the one of the BMS since an additional approximation is made. Overall, still an accurate prediction of the dispersion curves is obtained with a relative error smaller than $6.5 \cdot 10^{-2}$.

4 CONCLUSIONS

In this work, the BMS and GBMS unit cell model reduction techniques are extended towards 2D and 3D vibro-acoustic unit cell designs. A verification case shows that the methodologies are able to accelerate the vibro-acoustic dispersion curve calculation while maintaining an accurate prediction with respect to the full order model. Due to the accelerated performance assessment, the presented techniques are of particular interest during the design and tuning of periodic vibro-acoustic structures.

ACKNOWLEDGMENTS

The research of V. Cool (fellowship no. 11G4421N) and L. Van Belle (fellowship no. 1271621N) is funded by a grant from the Research Foundation - Flanders (FWO). Internal Funds KU Leuven are gratefully acknowledged for their support.

REFERENCES

[1] M.I. Hussein et al. Dynamics of phononic materials and structures: Historical origins, recent progress, and future outlook. *Applied Mechanics Review*, 66(4):040802, 2014.

[2] F. Bloch. Über die quantenmechanik der elektronen in kristallgittern. *Zeitschrift für Physik*, 52(7):555–600, 1929.

[3] O.R. Bilal, D. Ballagi, and C. Daraio. Architected lattices for simultaneous broadband attenuation of airborne sound and mechanical vibrations in all directions. *Physical Review Applied*, 10(5):054060, 2018.

[4] G. Li, Y. Chen, W. Chen, J. Liu, and H. He. Local resonance–Helmholtz lattices with simultaneous solid-borne elastic waves and air-borne sound waves attenuation performance. *Applied Acoustics*, 186:108450, 2022.

[5] D. Roca and M.I. Hussein. Broadband and intense sound transmission loss by a coupled-resonance acoustic metamaterial. *Physical Review Applied*, 16(5):054018, 2021.

[6] R.F. Boukadia, C. Droz, M.N. Ichchou, and W. Desmet. A Bloch wave reduction scheme for ultrafast band diagram and dynamic response computation in periodic structures. *Finite Elements in Analysis and Design*, 148:1–12, 2018.

[7] D. Krattiger and M.I. Hussein. Bloch mode synthesis: ultrafast methodology for elastic band-structure calculations. *Physical Review E*, 90(6), 2014.

[8] D. Krattiger and M.I. Hussein. Generalized Bloch mode synthesis for accelerated calculation of elastic band structures. *Journal of Computational Physics*, 357:183–205, 2018.

[9] R.R. Craig Jr and C.-J. Chang. Substructure coupling for dynamic analysis and testing. Technical report, NASA, 1977.

[10] M. Maess and L. Gaul. Substructuring and model reduction of pipe components interacting with acoustic fluids. *Mechanical Systems and Signal Processing*, 20(1):45–64, 2006.

[11] J. Herrmann, M. Maess, and L. Gaul. Substructuring including interface reduction for the efficient vibro-acoustic simulation of fluid-filled piping systems. *Mechanical Systems and Signal Processing*, 24(1):153–163, 2010.

[12] V. Cool, L. Van Belle, C. Claeys, E. Deckers, and W. Desmet. (Generalized) Bloch mode synthesis for the fast dispersion curve calculation of 3D periodic metamaterials. In *INTER-NOISE and NOISE-CON Congress and Conference Proceedings*, volume 263, pages 2102–2113. Institute of Noise Control Engineering, 2021.

[13] F.J. Fahy and P. Gardonio. *Sound and structural vibration: radiation, transmission and response, 2nd edition*. Elsevier, UK, 2007.

[14] C. Kittel. *Introduction to solid state physics*. Wiley New York, 2010.

[15] V. Cool, L. Van Belle, C. Claeys, E. Deckers, and W. Desmet. Impact of the unit cell choice on the efficiency of dispersion curve calculations using GBMS. *Journal of Vibration and Acoustics*, 2021.